BER Performance Comparison of Overlap FDE and Sliding-window Time-domain Equalization for Single-carrier Transmission

Tatsunori OBARA† Kazuki TAKEDA† and Fumiyuki ADACHI‡

Dept. of Electrical and Communication Engineering, Graduate School of Engineering, Tohoku University
6-6-05, Aza-Aoba, Aramaki, Aoba-ku, Sendai, 980-8579, JAPAN
E-mail: †{obara, kazuki}@mobile.ecei.tohoku.ac.jp ‡adachi@ecei.tohoku.ac.jp

***Abstract*— Minimum mean square error frequency-domain equalization (MMSE-FDE) can achieve a good performance in the case of single-carrier (SC) transmission in a frequency-selective fading channel. The conventional FDE requires the insertion of guard interval (GI) to avoid the inter-block interference (IBI). However, the GI insertion reduces the throughput. Recently, overlap FDE which requires no GI insertion was proposed. Another promising equalization technique which requires no GI insertion is sliding-window time-domain equalization (SWTDE). In this paper, we compare overlap FDE and SWTDE in terms of the bit error rate (BER) performance and computational complexity for single-carrier transmission.**

I. INTRODUCTION

The frequency-domain equalization (FDE) based on the minimum mean square error (MMSE) criterion can take advantage of the channel frequency-selectivity and achieve a good bit error rate (BER) performance in the case of single-carrier (SC) transmission[1]-[3]. The conventional FDE requires the insertion of guard interval (GI) to avoid the inter-block interference (IBI). However, this reduces the transmission throughput. In [4] and [5], overlap FDE which requires no GI insertion was presented. Overlap FDE can effectively suppress the residual IBI after FDE. It provides higher throughput than the conventional FDE [6]. Another promising equalization technique which requires no GI insertion is sliding-window time-domain equalization (SWTDE) based on MMSE criterion [7], [8]. It was shown in [7] that the SWTDE can achieve a good BER performance.

In this paper, we compare overlap FDE and SWTDE in terms of the BER performance and computational complexity for single-carrier transmission. We will show that, by extending the fast Fourier transform (FFT) block size, the residual IBI can be better suppressed and hence, overlap FDE can achieve almost the same BER performance as SWTDE with much less computational complexity.

The remainder of this paper is organized as follows. Section II presents the system model of single-carrier signal transmission using overlap FDE and SWTDE. In Sect. III, the BER performance and computation complexity comparisons are presented. Section IV offers some conclusions.

II. SYSTEM MODEL

A. Received signal representation

The transmitter and receiver structures are illustrated in Fig. 1. We assume a symbol-spaced L-path frequency-selective block fading channel. Throughout the paper, a symbol-spaced discrete-time representation is used. At the transmitter, the binary information sequence is data-modulated, and then the data-modulated symbol sequence $\{s(t);t=\ldots, -1, 0, 1, \ldots\}$ is transmitted without CP insertion. The transmitted symbol sequence $\{s(t);t=\ldots, -1, 0, 1, \ldots\}$ is received via a frequency-selective fading channel. The received signal sequence can be expressed as

$$r(t)=\sum_{l=0}^{L-1}h_l s(t-\tau_l)+\eta(t), \quad (1)$$

where h_l is the lth complex-valued path gain with $\sum_{l=0}^{L-1}E[|h_l|^2]=1$ ($E[.]$ denotes the ensemble average operation), and τ_l is the delay time of the lth path. $\eta(t)$ is a zero-mean complex-valued additive white Gaussian noise (AWGN) with a variance $2N_0/T_c$ with N_0 being the single-sided power spectrum density.

B. SWTDE [7], [8]

The received symbol sequence is divided into a sequence of M-symbol blocks. Then, the time-domain equalization is applied to an N_c-symbol block centering the M-symbol block of interest, where N_c ($>M$) is the equalization block length. After the equalization, the M-symbol block is picked up from the equalized N_c-symbol block to suppress the residual IBI. To equalize the next M-chip block, an N_c-symbol equalization window is shifted by M symbols as shown in Fig. 2.

The received N_c-symbol block is represented by vector $\mathbf{r}=[r(0), r(1)\ldots, r(N_c-1)]^T$ (the superscript T denotes the transpose operation). It can be expressed as

$$\mathbf{r}=\mathbf{h}_0\mathbf{s}_0+\mathbf{h}_{-1}\mathbf{s}_{-1}+\boldsymbol{\eta}, \quad (2)$$

where the first and second terms represent the desired signal component and the IBI component, respectively. $\mathbf{s}_0$, $\mathbf{s}_{-1}$ and $\boldsymbol{\eta}$ are $N_c\times 1$ vectors respectively given as

$$\begin{cases} \mathbf{s_0} = [s(0), s(1), \ldots, s(N_c - 1)]^T \\ \mathbf{s}_{-1} = [s(-N_c), s(-N_c + 1), \ldots, s(-1)]^T \\ \boldsymbol{\eta} = [\eta(0), \eta(1), \ldots, \eta(N_c - 1)]^T \end{cases} . \quad (3)$$

$\mathbf{h}_0$ and $\mathbf{h}_{-1}$ are $N_c \times N_c$ channel impulse response matrices given as

$$\begin{cases} \mathbf{h_0} = \begin{bmatrix} h_0 & & & \mathbf{0} \\ \vdots & \ddots & & \\ h_{L-1} & & \ddots & \\ & \ddots & & h_0 \\ & & \ddots \; \vdots \; \ddots & \\ \mathbf{0} & & h_{L-1} \cdots h_0 & \end{bmatrix} \\ \mathbf{h}_{-1} = \begin{bmatrix} & & h_{L-1} \cdots h_1 & \\ & & \ddots \; \vdots & \\ & & & h_{L-1} \\ & \mathbf{0} & & \end{bmatrix} \end{cases} . \quad (4)$$

TDE is carried on the received N_c-symbol vector $\mathbf{r}$ as

$$\hat{\mathbf{s}}_0 = \mathbf{W}\mathbf{r} , \quad (5)$$

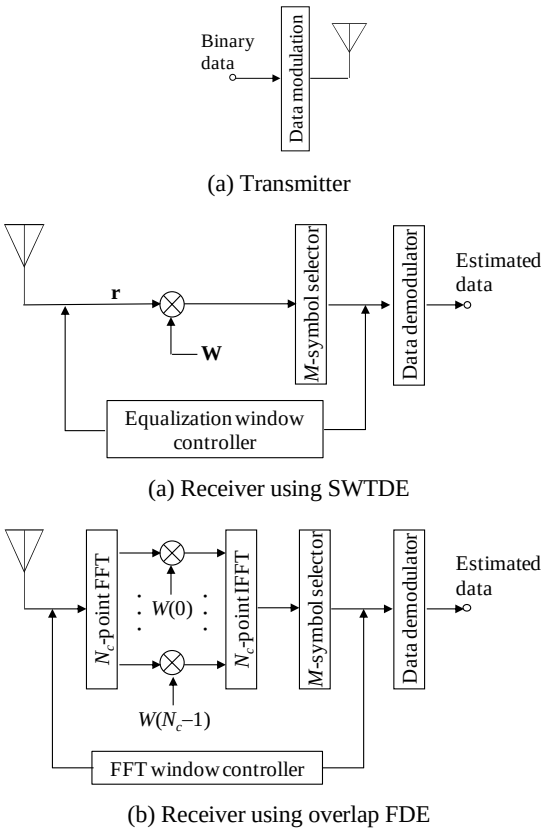

Fig. 1 Transmitter and receiver structures.

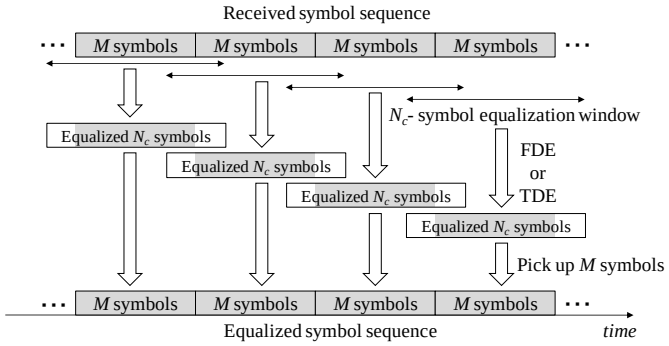

Fig. 2 Block signal processing of SWTDE and overlap FDE

where $\mathbf{W}$ is the $N_c \times N_c$ MMSE equalization weight matrix which minimizes the trace of the covariance matrix $E[\mathbf{e}\mathbf{e}^H]$ of the error vector $\mathbf{e} = \hat{\mathbf{s}}_0 - \mathbf{s}_0$. According to the Wiener theory [9], it is given as

$$\mathbf{W} = \boldsymbol{\Phi}_{SR}\boldsymbol{\Phi}_{RR}^{-1} = \mathbf{h}_0^H \left\{ \mathbf{h}_0\mathbf{h}_0^H + \mathbf{h}_{-1}\mathbf{h}_{-1}^H + \left(\frac{E_c}{N_0}\right)^{-1} \mathbf{I} \right\}^{-1} , \quad (6)$$

where $\boldsymbol{\Phi}_{SR}=E[\mathbf{s}_0\mathbf{r}^H]$ and $\boldsymbol{\Phi}_{RR}=E[\mathbf{r}\mathbf{r}^H]$. In Eq. (6), the superscript H denotes the Hermitian transpose operation. After TDE, only the central M-symbol block in the equalized N_c-symbol block is picked up.

C. Overlap FDE [4]-[6]

The residual IBI after MMSE-FDE is a circular convolution of the IBI and the impulse response of MMSE-FDE filter. The MMSE-FDE filter impulse response concentrates at a vicinity of time t=0. Therefore, the residual IBI is localized only near the both ends of the N_c-symbol block after MMSE-FDE. The overlap FDE is based on this observation [5]. The received symbol sequence is divided into a sequence of M-symbol blocks ($M<N_c$) similar to SWTDE. Then, N_c-point fast Fourier transform (FFT) is applied to an N_c-symbol block centering the M-symbol block of interest. After MMSE-FDE, the central M-symbol block in the equalized N_c-symbol block is picked up to suppress the residual IBI. The FFT intervals for consecutive M-symbol blocks are overlapped as shown in Fig. 2.

The received N_c-symbol block of Eq. (2) can be rewritten as

$$\mathbf{r} = \mathbf{h}\mathbf{s}_0 + \boldsymbol{\nu} + \boldsymbol{\eta} , \quad (7)$$

where the first term is the desired signal component and $\boldsymbol{\nu}$ denotes the IBI component expressed as $\boldsymbol{\nu}=\mathbf{h}_{-1}(\mathbf{s}_{-1}-\mathbf{s}_0)$. $\mathbf{h}$ is the $N_c \times N_c$ channel impulse response matrix given as

$$\mathbf{h}=\begin{bmatrix} h_0 & & & & h_{L-1} & \vdots \\ \vdots & \ddots & & & & h_{L-1} \\ h_{L-1} & & h_0 & \mathbf{0} & & \\ & \ddots & \vdots & \ddots & & \\ & & h_{L-1} & & h_0 & \\ & & & \ddots & \vdots & \ddots \\ \mathbf{0} & & & & h_{L-1} & \cdots \quad h_0 \end{bmatrix}. \qquad (8)$$

The received N_c-symbol block $\mathbf{r}$ is transformed by N_c-point fast Fourier transform (FFT) into the frequency-domain signal $\mathbf{R}=[R(0),R(1),...,R(N_c-1)]^T$. $\mathbf{R}$ is expressed as

$$\begin{aligned}\mathbf{R} &= \mathbf{Fr} \\ &= \mathbf{HS}+\mathbf{N}+\mathbf{\Pi}'\end{aligned} \qquad (9)$$

where $\mathbf{S}=\mathbf{Fs}_0$, $\mathbf{N}=\mathbf{F\nu}$, $\mathbf{\Pi}=\mathbf{F\eta}$ with $\mathbf{F}$ being the $N_c\times N_c$ FFT matrix given as

$$\mathbf{F}=\frac{1}{\sqrt{N_c}}\begin{bmatrix} e^{-j2\pi\frac{0\cdot 0}{N_c}} & e^{-j2\pi\frac{0\cdot 1}{N_c}} & \cdots & e^{-j2\pi\frac{0\cdot(N_c-1)}{N_c}} \\ e^{-j2\pi\frac{1\cdot 0}{N_c}} & e^{-j2\pi\frac{1\cdot 1}{N_c}} & \cdots & e^{-j2\pi\frac{1\cdot(N_c-1)}{N_c}} \\ \vdots & \vdots & \ddots & \vdots \\ e^{-j2\pi\frac{(N_c-1)\cdot 0}{N_c}} & e^{-j2\pi\frac{(N_c-1)\cdot 1}{N_c}} & \cdots & e^{-j2\pi\frac{(N_c-1)\cdot(N_c-1)}{N_c}} \end{bmatrix}. \qquad (10)$$

$\mathbf{H}$ is given as [10]

$$\mathbf{H}=\mathbf{FhF}^H=\begin{bmatrix} H(0) & & & \mathbf{0} \\ & \ddots & & \\ & & H(k) & \\ & & & \ddots \\ \mathbf{0} & & & H(N_c-1) \end{bmatrix}, \qquad (11)$$

where $H(k)=\sum_{l=0}^{L-1}h_l\exp\left(-j2\pi k\tau_l/N_c\right)$.

One-tap FDE is performed as

$$\hat{\mathbf{R}}=\mathbf{WR} \qquad (12)$$

where

$$\mathbf{W}=\begin{bmatrix} W(0) & & & \mathbf{0} \\ & \ddots & & \\ & & W(k) & \\ & & & \ddots \\ \mathbf{0} & & & W(N_c-1) \end{bmatrix} \qquad (13)$$

is the MMSE-FDE weight matrix with [9]

$$W(k)=\frac{H^*(k)}{|H(k)|^2+\Lambda^{-1}}. \qquad (14)$$

Λ is the signal-to-IBI plus noise power ratio (SINR) and $(.)^*$ denotes the conjugate operation.

The frequency-domain signal $\hat{\mathbf{R}}=[\hat{R}(0),\hat{R}(1),\ldots,\hat{R}(N_c-1)]^T$ after MMSE-FDE is transformed by N_c-point inverse FFT (IFFT) back to the time-domain signal $\hat{\mathbf{r}}=[\hat{r}(0),\hat{r}(1),\ldots,\hat{r}(N_c-1)]^T$ as

$$\hat{\mathbf{r}}=\mathbf{F}^H\hat{\mathbf{R}}. \qquad (15)$$

D. Computational complexity

SWTDE is time-domain equalization using a matrix computation and therefore, its computational complexity is very large. On the other hand, the complexity of overlap FDE is much smaller than SWTDE since FDE is one-tap equalization. Table 1 shows the number of complex multiply operations per symbol for SWTDE and overlap FDE. In SWTDE, due to the inverse matrix computation in Eq. (6), the number of multiply operations is in proportion to N_c^3 and therefore, the complexity significantly increases with N_c. Figure 4 compares overlap FDE and SWTDE in terms of the number of complex multiply operations per symbol. When N_c=128, the number of multiply operations is approximately 10^7 for SWTDE and 2×10^3 for overlap FDE; overlap FDE requires much less complexity than SWTDE.

Table 1 No. of complex multiply operations per symbol.

		No. of complex multiply operations per symbol
SWTDE	Weight generation	$5N_c^3/M$
	Chip equalization	N_c^2/M)
	Total	$(5N_c^3+N_c^2)/M$
Overlap FDE	N_c-point FFT	$(N_c\log_2N_c)/M$
	Weight generation	N_c/M
	FDE	N_c/M
	N_c-point IFFT	$(N_c\log_2N_c)/M$
	Total	$2N_c(1+\log_2N_c)/M$

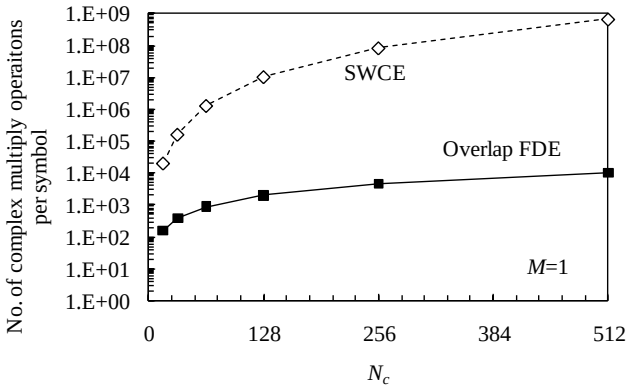

Fig. 4 Computational complexity comparison of overlap FDE and SWTDE

III. COMPUTER SIMULATION

We assume QPSK data-modulation. The propagation channel is assumed to be a frequency-selective block Rayleigh fading channel having a symbol-spaced L=16-path exponential

power delay profile with decay factor α. The ideal channel estimation is also assumed.

Figure 5 plots the BER performances of overlap FDE and SWTDE as a function of the average bit energy-to-noise power spectrum density ratio E_b/N_0(=0.5(E_s/N_0)) with M as a parameter. N_c=128 is assumed. Smaller M can provide better BER performance for both overlap FDE and SWTDE. However, when α=0dB (uniform power delay profile), overlap FDE is inferior to SWTDE even if small M is used. This is because the residual IBI is larger with overlap FDE than with SWTDE over an M-symbol block. When the channel frequency-selectivity is weak (α=6dB), the residual IBI becomes small and therefore, overlap FDE can achieve almost the same BER performance as SWTDE except for N_c=M.

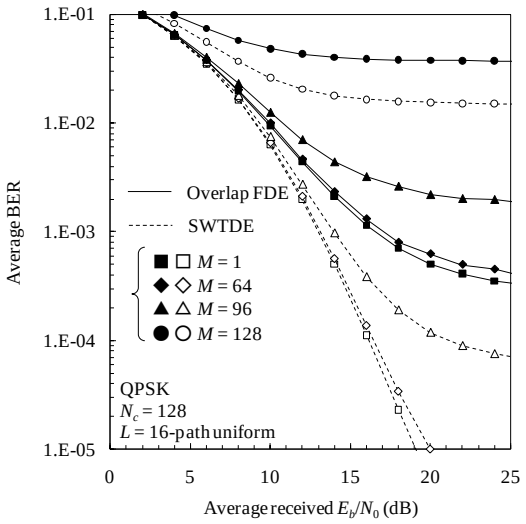

(a) α=0dB(uniform power delay profile)

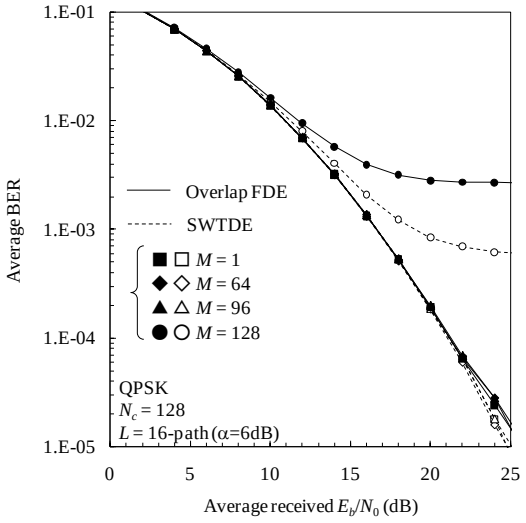

(b) α=6dB

Fig. 5 BER performance comparison for various values of M. N_c=128

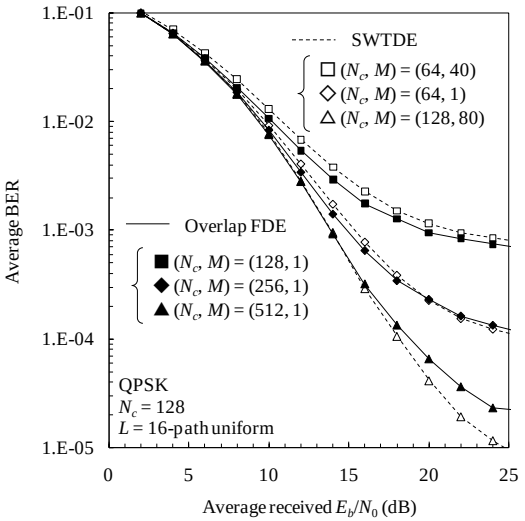

Fig. 6 BER performance comparison for various (N_c, M).

Overlap FDE can suppress more the residual IBI by increasing N_c while using the same value of M. Figure 6 plots the BER performance of overlap FDE when M=1 for various values of N_c and the BER performance of SWTDE for (N_c, M) = (64, 40), (64, 1) and (128, 80). The parameter settings (N_c, M) = (64, 80), (64, 1) and (128, 80) are found to minimize the computational complexity while achieving almost the same performance as overlap FDE. They are used to measure the BER performance of SWTDE plotted in Fig. 6. When N_c=128, 256 and 512, the number of multiply operations per symbol is about 2×10^3, 5×10^3, and 1×10^4, respectively, for overlap FDE while it is 3×10^4, 1×10^6, and 1×10^5, respectively, for SWTDE using (N_c, M) = (64, 40), (64, 1) and (128, 80). As a consequence, overlap FDE can achieve almost the same performance as SWTDE with much less complexity.

IV. CONCLUSION

In this paper, we compared overlap FDE and SWTDE in terms of the BER performances and computational complexity for single-carrier transmission. In the case of overlap FDE, the residual IBI still exists. However, by extending the FFT block size, the residual IBI can be better suppressed and therefore, overlap FDE can achieve almost the same performance as SWTDE with much less complexity than SWTDE.

REFERENCES

[1] D. Falconer, S. L. Ariyavisitakul, A. Benyamin-Seeyar, and B. Eidson, "Frequency domain equalization for single-carrier broadband wireless systems," IEEE Commun., Vol. 40, No.4, pp 58-66, Apr. 2002.

[2] M. V. Clark, "Adaptive frequency-domain equalization and diversity combining for broadband wireless communications," IEEE J. Select. Areas. Commun., Vol. 16, No. 8, pp. 1385-1395, Oct.1998.

[3] F. Adachi, D. Garg, S. Takaoka, and K. Takeda, "Broadband CDMA techniques," IEEE Wireless Commun., Vol. 12, No.2, pp.8-18, Apr. 2005.

[4] I. Martoyo, T. Weiss, F. Capar, and F. K. Jondral, "Low complexity CDMA downlink receiver based on frequency domain equalization," IEEE Vehicular Technology Conference (VTC) '03 fall, Orlando, Florida, USA, Sept. 2003.

[5] T. Takeda, H. Tomeba, and F. Adachi, "Iterative overlap FDE for DS-CDMA without GI," IEEE 64th VTC, Montreal, Quebec, Canada, Sept. 2006.

[6] Kazuki Takeda, Hiromichi Tomeba, Kazuaki Takeda and Fumiyuki Adachi, "DS-CDMA HARQ with Overlap FDE," IEICE Trans. Commun., Vol. E90-B, No. 11, pp. 3189-3196, Nov. 2007.

[7] A. Klein, "Data Detection Algorithms Specially Designed for the Downlink of Mobile Radio Systems," IEEE VTC'97-Spring, Phoenix, May 1997.

[8] T. Kawamura, Y. Kishiyama, K. Higuchi, and M. Sawahashi, "Comparison Between Multipath Interference Canceller and Chip Equalizer in HSDPA in Multipath Channel," IEEE VTC2002-Spring, Birmingham, May 2002.

[9] S. Haykin, *Adaptive Filter Theory*, 4th ed., Prentice Hall, 1996.

[10] G. H. Golub and C. F. van Loan, *Matrix Computations*, 3rd ed. Baltimore, MD, Johns Hopkins Univ. Press, 1996.